



---

# Audio Engineering Society

# Convention Paper

Presented at the 121st Convention  
2006 October 5–8 San Francisco, CA, USA

*This convention paper has been reproduced from the author's advance manuscript, without editing, corrections, or consideration by the Review Board. The AES takes no responsibility for the contents. Additional papers may be obtained by sending request and remittance to Audio Engineering Society, 60 East 42<sup>nd</sup> Street, New York, New York 10165-2520, USA; also see [www.aes.org](http://www.aes.org). All rights reserved. Reproduction of this paper, or any portion thereof, is not permitted without direct permission from the Journal of the Audio Engineering Society.*

---

## Addendum<sup>1</sup>

### An Important Aspect of Underhung Voice-Coils: A Technical Tribute to Ray Newman

Raymond J. Newman (deceased)<sup>1</sup>, D. B. (Don) Keele, Jr.<sup>2</sup>, David E. Carlson<sup>3</sup>, Jim Long<sup>4</sup>, Kent H. Frye<sup>5</sup>, Matthew S. Ruhlen<sup>6</sup>, and John Sheerin<sup>6</sup>

<sup>1</sup> Electro-Voice Inc., Buchanan, MI, 49107 USA (As of 1992)

<sup>2</sup> Harman International Industries, Martinsville, IN, 46151 USA  
DKeele@Harman.com

<sup>3</sup> Electro-Voice, Div. Telex Communications, Burnsville, MN, 55337 USA  
DE.Carlson@US.Telex.com

<sup>4</sup> Electro-Voice, Div. Telex Communications, Burnsville, MN, 55337 USA  
JJimLong@cs.com

<sup>5</sup> Gentex Corporation, Fire Protection Group, Zeeland, MI, 49464 USA  
KFrye@Gentex.com

<sup>6</sup> Harman/Becker Automotive Systems, Martinsville, IN, 46151 USA  
MRuhlen@HarmanBecker.com  
JSheerin @HarmanBecker.com

#### ABSTRACT

This addendum adds additional research and information to the original paper and also adds an additional co-author (John Sheerin, who ran all the magnetic simulations). This research includes: plots of BI force factor versus displacement for each of the simulated motor structures, a definition of a new type underhung motor structure with an example, a definition with results of a motor structure figure of merit (FOM) number, and three new data tables which include core physical volume and relevant FOM numbers. This additional information was not discussed in Ray Newman's original memos, but is reported here as a logical extension of his research. It was revealed that the BI-factor decreases much less rapidly when the voice-coil leaves the gap in the underhung structure as compared to the overhung structure. This led to the introduction of a new style underhung motor type where the voice-coil is deliberately allowed to come partially out of the gap at high excursions. The Type 1 underhung motor is the traditional structure where the voice-coil is confined to the gap even for the largest excursions. The Type 2 underhung motor structure allows the voice-coil to partially leave the gap for large excursions. Although the Type 1 underhung structure exhibits extreme linearity of BI factor versus displacement and as a result exhibits low distortion, the Type 2 motor relaxes the BI-factor linearity and distortion requirements and trades them off for greater excursion capability. The Type 2 motor exhibits high linearity for low to moderate excursions, and less linearity for higher excursions. The FOM of the Type 2 underhung structure is significantly higher than the equivalent overhung structure with the same voice-coil, efficiency and Xmax.

---

<sup>1</sup>A PDF copy of this addendum may be requested from coauthor Don Keele via an e-mail (DKeele@Harman.com).

## 1. INTRODUCTION

This is an addendum to the paper “An Important Aspect of Underhung Voice-Coils: A Technical Tribute to Ray Newman.” This addendum adds additional information to the paper by extending Newman’s research beyond that which he reported in his original memos. This information includes plots of BI force factor versus displacement for each of the simulated motor structures, a definition of a new type of underhung motor structure with an example, definition and results of a motor structure figure of merit (FOM) number, and three new motor structure data tables which include core physical volume and relevant FOM numbers.

In the original paper, the decision was made (somewhat naively) to not include plots of BI force factor versus voice-coil displacement because the plots of BI versus position in the gap appeared to be so well behaved (see even numbered figures from 18 to 28 in the original paper). When these plots were generated, several unexpected features resulted. The major feature revealed was that the skirts of the BI versus displacement plots roll off much less rapidly for the underhung structure than the overhung structure. This means that the effective maximum excursion for a particular droop in BI factor, is much greater for the underhung motor than the overhung motor.

This lead to the definition of a new underhung motor type where the voice-coil is deliberately allowed to come partially out of the gap at high excursions. The Type 1 underhung motor is the traditional very-linear structure where the voice-coil is confined to the gap even for the largest excursions. The new Type 2 underhung motor structure allows the voice-coil to partially leave the gap for large excursions. The latter underhung motor type relaxes the extreme BI-factor versus displacement linearity of the Type 1 structure and trades it off for greater excursion capability. The Type 2 underhung motor exhibits high linearity for low to moderate excursions, and less linearity for higher excursions.

This addendum also defines a motor structure figure of merit (FOM) for comparing different types of motor structures. The FOM is directly proportional to electro-magnetic damping factor and maximum excursion, and inversely proportional to total magnetic energy required and core physical volume.

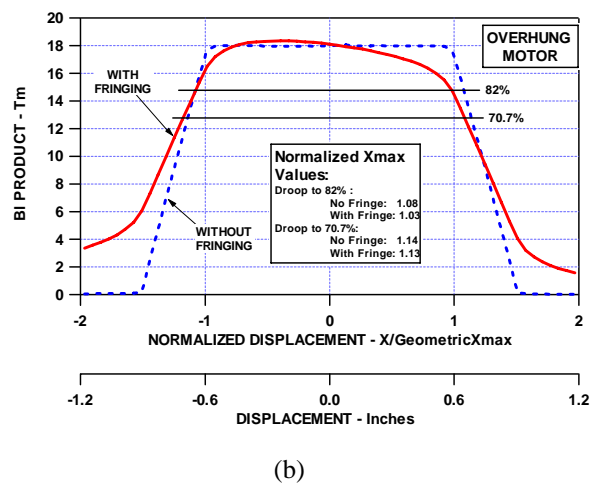
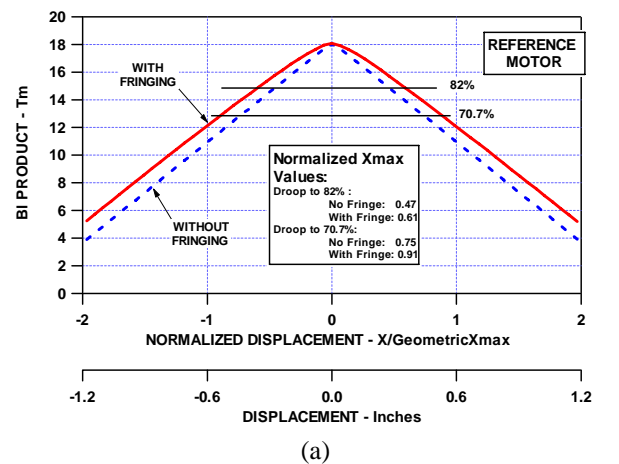
Analysis reveals that the FOM of the Type 2 underhung structure is significantly higher than the equivalent overhung structure with the same voice-coil, efficiency and  $X_{max}$ .

## 2. BL FORCE FACTOR VERSUS VOICE-COIL DISPLACEMENT

In this section, the BI force factor versus voice-coil displacement is plotted for the three motor structures analyzed in the original paper: reference, overhung, and underhung. Each graph plots the BI versus displacement for the CASE 1 (perfect soft magnetic material and no fringing) and CASE 3 (pure iron soft magnetic material with fringing) simulation situations. Each graph has horizontal lines drawn at the levels where the BI sags to 82% and 70.7% respectively of the rest-position BI. The 82% droop level is one suggested by Klippel by considering distortion[1].

Remember that a BI versus displacement plot is generated by convolving the flux density ( $B$ ) versus position plot with a rectangular voice-coil function.

The BI versus displacement plots are shown in the next figure (Fig. 1): reference (a), overhung (b), and underhung (c).



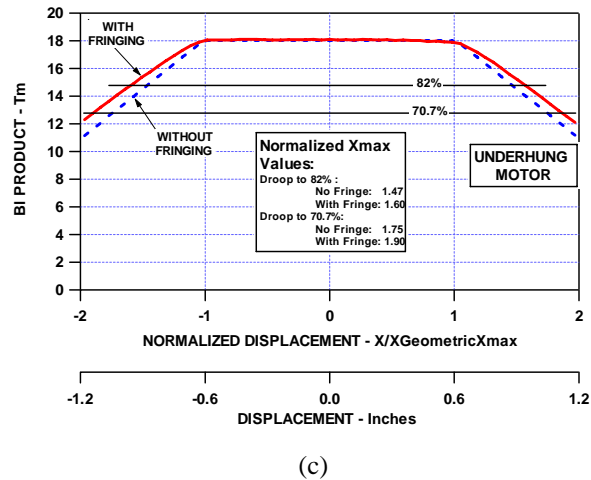


Fig. 1. BI force factor versus voice-coil displacement for each of the three motor structures analyzed in the original paper. (a) Reference. (b) Overhung. (b) Underhung. All three structures house the same 1.5" voice-coil but have different top plate thicknesses: 1.5" (a), 0.3" (b), and 2.7" (c). All were designed to have a BI of 18 T-m at zero displacement. Two curves are shown: without fringing (CASE 1: dashed), and with fringing (CASE 3: solid). Horizontal lines are drawn at the 82% and 70.7% BI droop levels. Two displacement scales are displayed under each graph: a displacement scale normalized to the designed geometric  $X_{\max}$  of 0.6", and a displacement scale in inches. The box indicates the normalized  $X_{\max}$  values at the 70.7% and 82% droop levels for both the fringe and no fringe curves.

## 2.1. Observations

### 2.1.1. Reference Structure

Figure 1(a) shows the results for the reference motor whose top plate thickness (gap) is equal to the voice-coil length. Note the distinctive pyramidal shape with straight sides. The BI starts to immediately decrease as the voice-coil starts moving out of the gap. The fringe (solid curve) raises the skirts of the BI curve and somewhat increases the displacement at the 70.7% or 82% droop levels (+21% and +30% respectively).

Note the gradual rolloff of BI as the voice-coil moves out of the gap. Convolution theory states that the "no fringe" BI curve (dashed curve) should fall to zero when the voice-coil just leaves the gap completely. For this example, this occurs at a displacement of  $\pm 1.5$  inches or a normalized displacement of  $\pm 2.5$ . (Side note: this zero-BI displacement value is just simply one half of the sum of the voice-coil length and the top plate thickness). The calculated skirt rolloff slope is 7.2 T-m (18/2.5) per unit normalized displacement.

Note that with fringe (solid curve), the 70.7% BI droop excursion is only slightly less (about 10%) than the designed geometric  $X_{\max}$  of the overhung and underhung motors!

### 2.1.2. Overhung Structure

Figure 1(b) shows the results for the overhung motor. Without fringe (dashed curve), the BI curve exhibits a flat region between normalized displacement values of  $\pm 1$  and then rolls off linearly to zero at a displacement of  $\pm 0.9$ " (normalized displacement of 1.5). This corresponds to a high skirt rolloff slope of 36 T-m (18/0.5) per unit normalized displacement. Note that this is a five times higher rolloff rate than the reference motor (a)!

With fringe (solid curve), the BI curve exhibits a definite asymmetry with higher BI going into the gap and less going out. This is because the fringe field is stronger inside the structure than outside. Interestingly when fringe is added, the maximum displacement at the 70.7% and 82% droop levels actually decreases slightly (-1% and -5% respectively)! Note also that because of the much higher rolloff rate of the skirts, the maximum excursion at the 70.7% and 82% droop levels (with fringe) is only about 13% and 3% (respectively) greater than the designed geometric  $X_{\max}$ .

### 2.1.3. Underhung Structure

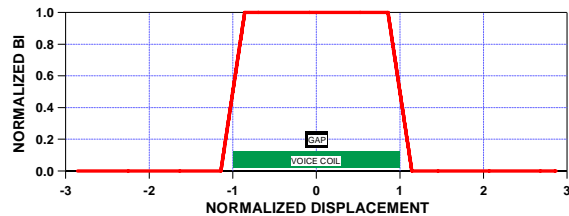
Figure 1(c) shows the results for the underhung motor of the original paper. Immediately apparent is the much lower skirt roll off rate as compared to the overhung motor. Both the "with fringe" (solid curve) and "without fringe" BI curves are absolutely flat between normalized displacement values of  $\pm 1$  and then rolloff linearly beyond. Without fringe, the curves fall to zero at a displacement of  $\pm 2.1$ " (normalized displacement of 3.5) with a rolloff slope of 7.2 T-m (18/2.5) per unit normalized displacement.

Unexpectedly, this is exactly the same rolloff rate as the previous reference structure (a). Because of this low rolloff rate, the maximum excursion at the 70.7% and 82% droop levels is an extremely generous 60% and 90% (respectively) greater than the designed geometric  $X_{\max}$ . This implies that the maximum excursion of the underhung structure can be greatly increased if the voice-coil is allowed to partially leave the gap. This fact led to the definition of the new type underhung structure described in the following section 4.

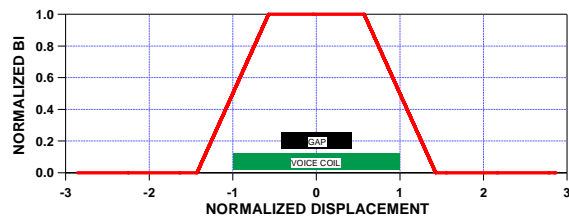
### 3. BL VERSUS DISPLACEMENT: VARY TOP PLATE THICKNESS

This section investigates how the shape of the BL versus displacement curve changes for different ratios of voice-coil length to top plate thickness. The graphs were generated by mathematically convolving a rectangular voice-coil function with a rectangular gap B versus position function.

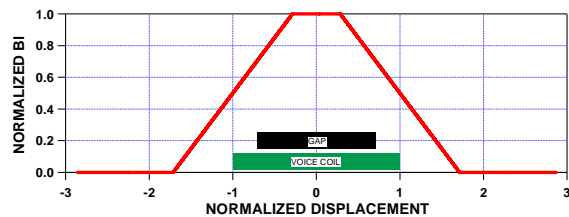
The ratio was varied by maintaining a constant voice-coil length and varying the top-plate thickness over a wide range from overhung to underhung. Seven ratio values of top-plate thickness to voice-coil length were chosen for simulation:  $1/7$  (maximum overhung, i.e. the top plate thickness is  $1/7^{\text{th}}$  the voice-coil length),  $3/7$ ,  $5/7$ ,  $7/7$  (voice-coil equal to top-plate thickness),  $9/7$ ,  $11/7$ , and  $13/7$  (maximum underhung). These fractional values corresponded to decimal values of 0.14, 0.43, 0.71, 1.00, 1.29, 1.57, and 1.86. The BL factor was held constant at a normalized value of unity.



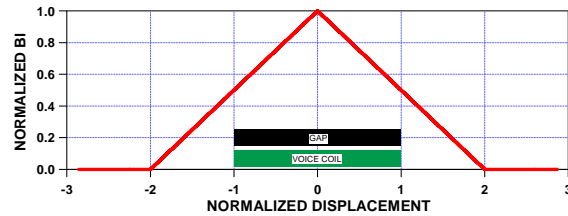
(a)



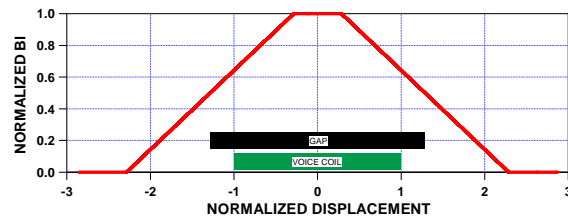
(b)



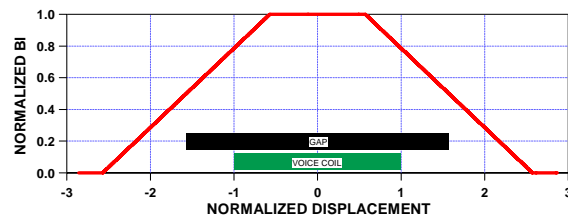
(c)



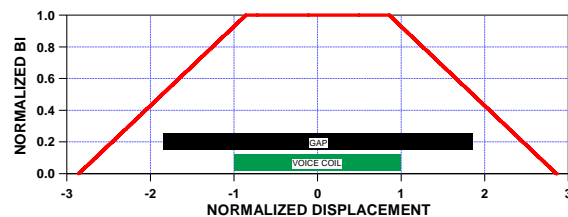
(d)



(e)



(f)



(g)

Fig. 2. Series of BL force factor versus voice-coil displacement graphs illustrating how the shape changes for different ratios of voice-coil length to top plate thickness. The ratio is varied by maintaining a constant voice-coil length and varying the top-plate thickness. (a) Top plate thickness =  $1/7^{\text{th}}$  the voice-coil length (maximum overhung). (b)  $3/7^{\text{th}}$ . (c)  $5/7^{\text{th}}$ . (d)  $7/7^{\text{th}}$  (voice-coil equal to top-plate thickness), (e)  $9/7^{\text{th}}$ . (f)  $11/7^{\text{th}}$ . (g)  $13/7^{\text{th}}$  (maximum underhung). The relative sizes of the voice-coil and top plate (gap) are indicated with horizontal bars on the bottom of the graph: top black bar: gap, bottom green bar: voice-coil. Note that the slope of the rolloff changes when the gap length is less than the voice-coil length (a – c), but remains the same for gap lengths greater than or equal to the voice-coil length (d – g).

### 3.1. Observations

In the overhung range (Fig. 2a to 2c) where the voice-coil is longer than the gap, the rate at which the BI drops when the voice-coil leaves the gap increases the more the amount of overhang, i.e. the skirt slope increases as the gap becomes smaller. In contrast with this, in the equal or underhung range (Fig. 2d to 2g) where the voice-coil is equal to or shorter than the gap, the skirt rolloff rate is independent of the amount of underhang and significantly less than the overhung values.

(Side note: the skirt falls to zero in a distance equal to the shortest of the two functions being convolved. In the overhung case, the gap is the shortest and changes with the size ratio. In the underhung case, the voice-coil is the shortest but does not change with the size ratio.)

This implies that if the voice-coil is allowed to partially leave the gap in the underhung structure, significant increases in maximum excursion can be realized as compared to the overhung structure. This observation led to the definition of the new type underhung structure described in the following section.

## 4. DEFINE UNDERHUNG TYPE 1 AND UNDERHUNG TYPE 2 MOTORS

This section defines a new underhung motor structure that allows the voice-coil to partially leave the gap. Two underhung types are defined: Type 1 is the conventional structure where the voice-coil is confined to the gap even for the largest excursions, and Type 2 is the structure that allows the voice-coil to partially leave the gap for large excursions. The Type 2 structure relaxes the extreme BI-factor linearity of Type 1 and trades it off for greater excursion capability and higher distortion for larger excursions.

In effect, the Type 2 motor exhibits high linearity for low to moderate excursions, and less linearity for higher excursions. As compared to Type 1, the Type 2 BI vs. displacement curve exhibits a narrower region where the BI is flat, and then commences a gradual rolloff down to the specified amount of BI droop. Often, this a very good match to typical bass program material that exhibits an amplitude histogram that spends most of its time around low amplitude values.

The following BI versus displacement graph (Fig. 3), shows the results of a Type 2 underhung structure designed to have the same maximum excursion at the 70.7% BI droop level (normalized  $X_{max}$  of 1.13) as the overhung structure described in the original paper and here in Fig. 1b. As before, the structure uses the same

voice-coil as all the previous motors and is setup to yield the same BI product for small displacements (BI = 18 T-m at the peak of the graph).

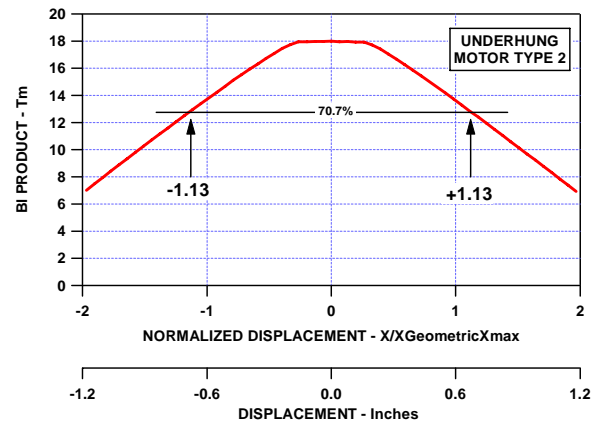


Fig. 3. BI force factor versus voice-coil displacement for the underhung Type 2 structure designed to have the same maximum displacement as the overhung motor of Fig. 1b at the 70.7% BI droop level (a CASE 3 normalized  $X_{max}$  of 1.13 or actual  $X_{max}$  of 0.68"). Note that the BI versus displacement shape is very flat between normalized displacements of  $\pm 0.3$  and then falls gradually to the 70.7% level at a BI of 12.7 T-m.

For reference and comparison purposes, the following graph (Fig. 4) shows the BI versus displacement plots of all four structures plotted on the same graph.

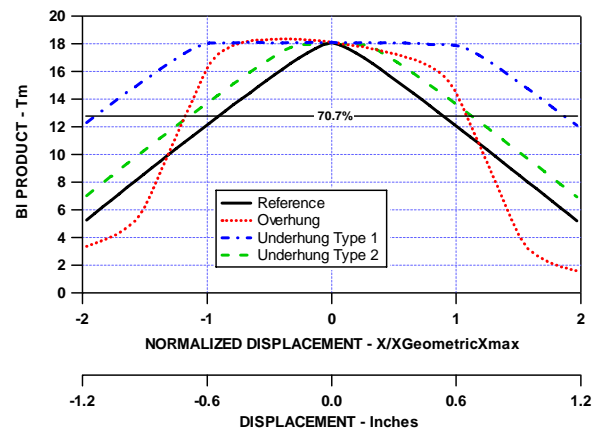


Fig. 4. BI force factor versus voice-coil displacement plots for the four motors analyzed in this addendum (all CASE 3 with pure iron core and fringe). Reference (solid black). Overhung (dotted red). Underhung Type 1 (dot-dash blue). Underhung Type 2 (dashed green).

### 5. MAXIMUM EXCURSIONS

This section shows scaled drawings of each of the analyzed motor structures with the maximum, minimum, and rest positions of the voice-coil indicated. Also indicated are the relevant  $X_{max}$  values and top plate (gap) thickness.

The first subsection shows the drawings for the two motors analyzed in the original paper which were designed to have equal geometric  $X_{max}$  values.

The second subsection shows drawings of the three motors analyzed in the original paper (reference, overhung, and underhung) plus the new underhung Type 2 structure defined in this addendum. Here  $X_{max}$  is defined at the excursion level where the BI droops to 70.7% of its rest position. This level is attained only if the voice-coil is allowed to partially leave the gap.

#### 5.1. Maximum Geometric Excursion

The following figure (Fig. 5) shows drawings of the overhung and underhung motor structures analyzed in the original paper with the geometric  $X_{max}$  values and top plate (gap) thicknesses indicated. These drawings are included here for reference and are essentially duplicates of Fig. 3 in the original paper.

Note that the geometric  $X_{max}$  definition forces the gap to either be completely filled with a portion of the voice-coil (overhung) or must contain the complete voice-coil (underhung). The voice-coil is not allowed to partially leave the gap. Both structures were designed to have the same geometric  $X_{max}$  of 0.6". The reference structure is not shown here because it has equal voice-coil and top plate lengths and thus has a geometric  $X_{max}$  of zero.

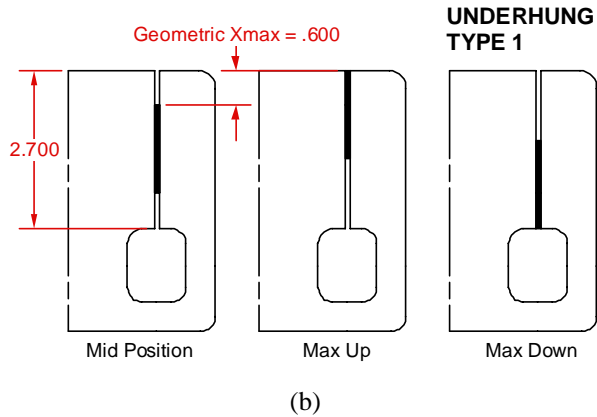
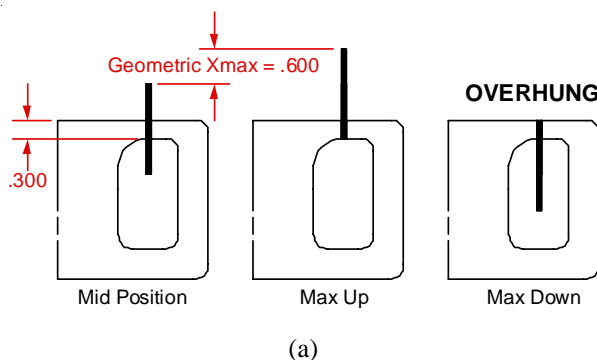
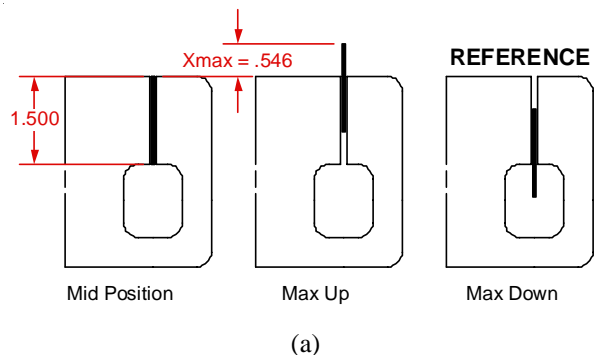


Fig. 5. Maximum voice-coil excursions for the overhung (a.) and underhung Type 1 (b.) motor structures with the geometric  $X_{max}$  indicated. Both motors were designed to have the same geometric  $X_{max}$  of 0.600". The top plate thickness is indicated on each drawing. The drawings have the same scale as the structures used in the simulations of this paper. Only the right half of the axially symmetric structure is shown. Mid position (left), maximum up position (middle), and maximum down position (right). All dimensions in inches. This figure essentially repeats Fig. 3 of the original paper and is included here for reference and comparison. All dimensions in inches.

#### 5.2. Maximum Excursion for BI Droop to 70.7%

Fig. 6 (following) shows depictions of the three motor structures analyzed in the original paper (reference, overhung, and underhung) and the underhung Type 2 structure defined in this addendum. The mid, maximum up, and maximum down positions of the voice-coil are shown for each motor. All the structures allow the voice-coils to partially leave the gap so that the BI can sag to the 70.7% level. It is at this displacement that  $X_{max}$  is defined. Here the original underhung structure is called a Type 1 motor.



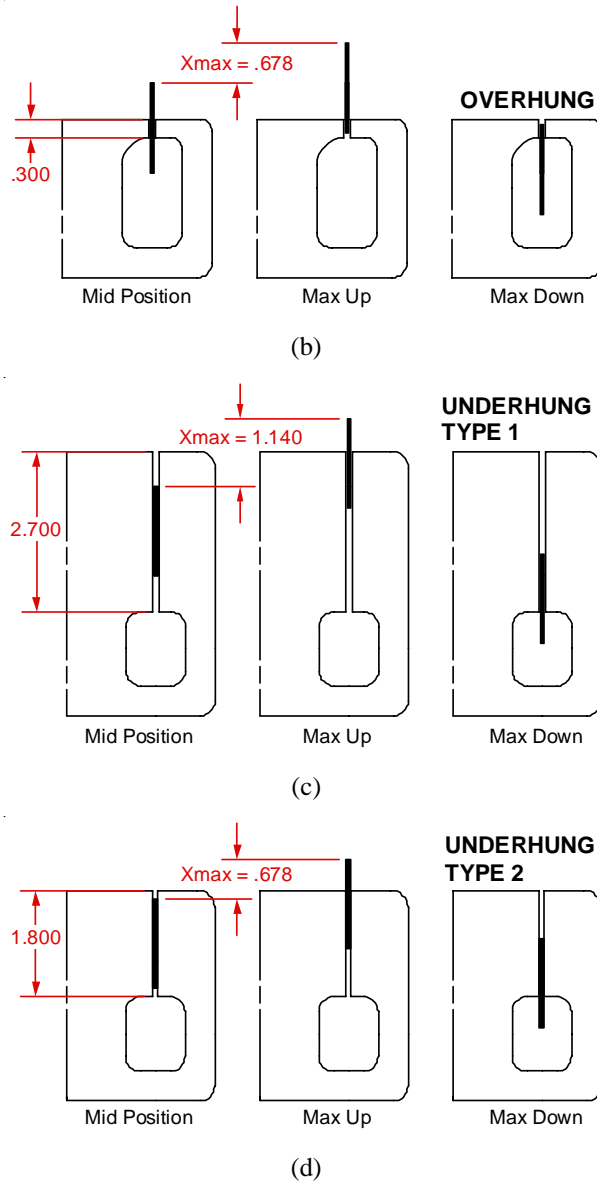


Fig. 6. Maximum voice-coil excursions for the reference (a), overhung (b), underhung Type 1 (c), and underhung Type 2 (d) motor structures allowing the  $Bl$  force factor to sag to a level that is 70.7% of the rest position. Note that all voice-coils have to partially leave the gap so that the  $Bl$  is reduced. Note that all the motors contain identical 1.5"-long voice-coils, but with varying top-plate thicknesses and  $X_{max}$  values which are indicated on each drawing. Note also that the underhung Type 2 motor (d) has been designed to have the same  $X_{max}$  as the overhung motor (b). The drawings have the same scale as the structures used in the simulations of this paper. Only the right half of the axially symmetric structure is shown. Mid position (left), maximum up position (middle), and maximum down position (right). All dimensions in inches.

## 6. ADDITIONAL MOTOR STRUCTURE SIMULATION DATA

This section essentially repeats one of the motor structure simulation data tables of the original paper but with data on the new underhung Type 2 structure. The table also includes a new column giving the motor's physical core volume. The core volume is included as a factor in the calculation of the structure's figure of merit (FOM) described in the next section.

This parameter list repeats the list of the original paper for reference but adds the additional core physical volume parameter (item 5). The motor parameters listed in the table include:

1. electromagnet MMF,
2. average flux density in gap (averaged along a line in the center of the gap from one edge of the gap to the other),
3.  $Bl$  product,
4. core flux,
5. core physical volume,
6. gap reluctance,
7. core reluctance,
8. total reluctance,
9. gap magnetic energy,
10. core magnetic energy,
11. fringe magnetic energy, and
12. total magnetic energy.

These parameters are shown in table 1 located at the end of this addendum. All the motors analyzed in the table were designed to have a rest  $Bl$  value of 18 T-m and use the same voice-coil, thus the electromagnetic damping factor ( $(Bl)^2/R_e$ ) of the motors are all equal.

As you might recall from the original paper, this value of  $Bl$  forced the total magnetic energy requirements of the original overhung and underhung motors to be equal. The underhung motor requires less magnet energy than the overhung for  $Bl$ s lower than 18 T-m and more magnet for  $Bl$ s higher.

## 7. FIGURE OF MERIT (FOM)

This section defines a motor structure figure of merit (FOM) and then applies it to the motor structures of the original paper and then to the motors defined here in the addendum. Bar charts with normalized FOM values are shown for each motor.

## 7.1. Definition

The definition incorporates the following motor parameters:

1. Electro-magnetic damping factor  $\left(\frac{(Bl)^2}{R_e}\right)$ ,
2. Maximum excursion ( $X_{\max}$ ),
3. Total magnetic energy ( $E_{TM}$ ), and
4. Physical core volume ( $V_C$ ).

The FOM is directly proportional to parameters 1 and 2, and inversely proportional to 3 and 4 as follows:

$$\begin{aligned} \text{FOM} &= \frac{\text{ElectroMagneticDamping} \times \text{MaximumExcursion}}{\text{TotalMagneticEnergy} \times \text{CoreVolume}} \\ &= \frac{\left(\frac{(Bl)^2}{R_e}\right) X_{\max}}{E_{TM} V_C} = \frac{(Bl)^2 X_{\max}}{R_e E_{TM} V_C} \end{aligned} \quad (1)$$

Parameter 1, the electro-magnetic damping factor, directly sets the small-signal efficiency of the loudspeaker (the higher the better). Parameter 2, the maximum excursion, is a large-signal parameter which indicates how far the loudspeaker's cone can move and therefore its air-moving capability (the higher the better). Parameter 3, the total magnetic energy, is an indicator of how much magnet (hence cost) is required to supply all the magnetic needs of the motor structure including the gap, core loss, and fringe loss (the lower the better). Parameter 4, the physical core volume, indicates how much iron or steel is required for the motor's magnetic path (the lower the better).

## 7.2. Figure of Merit for Geometric $X_{\max}$ Motors

This section shows the results of FOM calculations for the three motor structures of the original paper (reference, overhung, and underhung). All FOM data is normalized to the FOM of the overhung structure. The overhung and underhung (called Type 1 here) structures were designed to have the same geometric  $X_{\max}$ . Note that the geometric  $X_{\max}$  of the reference motor is zero by definition, and therefore its FOM is also zero. Note that because each structure uses the same voice-coil and has the same Bl force factor (18 T-m), all have identical electro-magnetic damping factors.

The bar charts in Fig. 7 (following), show the FOM of these three structures both excluding (a) and including (b) the core volume factor. Table 2 at the end of this addendum contains numbers for  $X_{\max}$  and FOM for these three structures.

### 7.2.1. Exclude Core Physical Volume

Excluding core physical volume (Fig. 7a), the overhung and underhung structures have identical FOMs. The FOM in this case depends only on the motor's total magnetic energy which are made equal by the specific choice of Bl product. As noted before, the reference motor's FOM is zero because it has no excursion (by definition).

### 7.2.2. Include Core Physical Volume

If core volume is included (Fig. 7b), the FOM of the underhung structure drops to 0.47 times that of the overhung structure. The reference motor's FOM is still zero. This implies that if structure weight and size are important the overhung motor wins out over the underhung motor if the excursion is limited to geometric  $X_{\max}$  values.

Note that the original paper pointed out that if the Bl product is lower than 18 T-m, the underhung motor actually requires less magnet energy than the overhung motor. This will increase the FOM of the underhung motor as compared to the overhung motor, and thus the choice between the two structures may change.

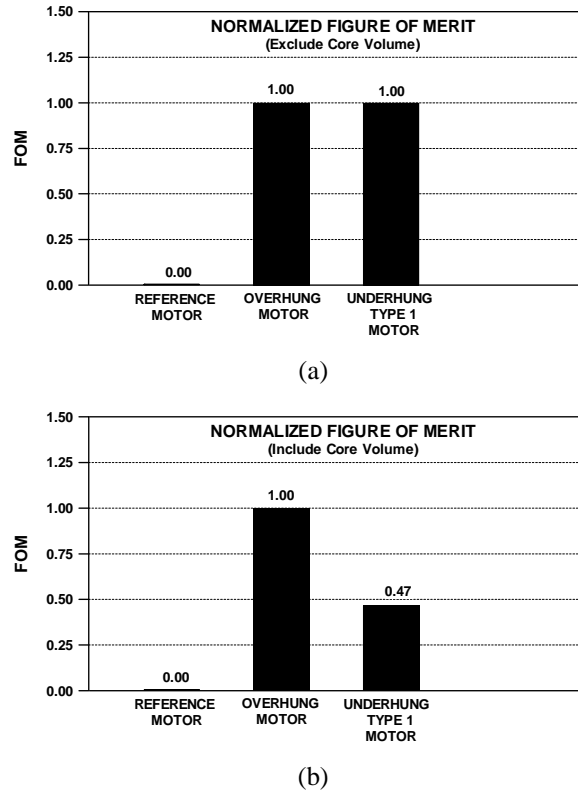


Fig. 7. Figure-of-merit bar charts for the three motor structures of the original paper (reference, overhung, and underhung Type 1). All structures uses identical voice-coils and are designed to have the same rest BI of 18 T-m. Remember that this value of BI forced the magnetic requirements of the overhung and underhung motors to be equal. These three structures were designed to meet geometric  $X_{\max}$  requirements. (a) excluding core physical volume. (b) including core physical volume. The reference motor has zero FOM by definition because it has zero geometric  $X_{\max}$ . When core volume is included (b), the FOM of the underhung motor drops.

### 7.3. Figure of Merit for a 70% BI Droop $X_{\max}$

This section shows the results of FOM calculations for the four motor structures of this addendum (reference, overhung, underhung Type 1, and underhung Type 2). All these structures allow the voice-coils to partially leave the gap so that the BI can sag to the 70.7% level. It is at this displacement that  $X_{\max}$  is defined. All FOM data is normalized to the FOM of the overhung structure.

Two bar charts are shown in the following Fig. 8, one excluding the core volume FOM factor (a), and one including the core volume factor (b). Note that the  $X_{\max}$  of the underhung Type 2 structure was designed to have the same  $X_{\max}$  as the overhung structure. The  $X_{\max}$  values of the remaining two structures are different.

Table 3 at the end of this addendum contains  $X_{\max}$  and FOM numbers for the four structures with and without core volume considered in the calculations.

#### 7.3.1. Exclude Core Physical Volume

Excluding core physical volume (Fig. 8a), the underhung Type 2 motor has the highest FOM, but only slightly higher (8%) than the reference motor. Both are roughly two and half times higher than the overhung motor! Note that the FOM of the underhung Type 1 motor is nearly 70% greater than the overhung motor. This means that the extreme linearity and very-high excursion of the underhung motor comes without penalty if core volume and motor depth are not a problem.

#### 7.3.2. Include Core Physical Volume

If core volume is included in the FOM calculations (Fig. 8b), the FOMs of the reference and two underhung motors drop significantly as compared to the overhung motor. This is because the overhung motor has the lowest core volume of the four structures and thus is given more weight in the FOM calculations.

Even with core volume included, the reference and underhung Type 2 motors still have roughly 60% higher FOM values than the overhung motor. Note that the FOM of the underhung Type 1 motor has dropped below the overhung motor, but is only 20% less. This indicates that the large excursion and noteworthy linearity of the underhung motor can be utilized without significant disadvantage as compared to the overhung structure.

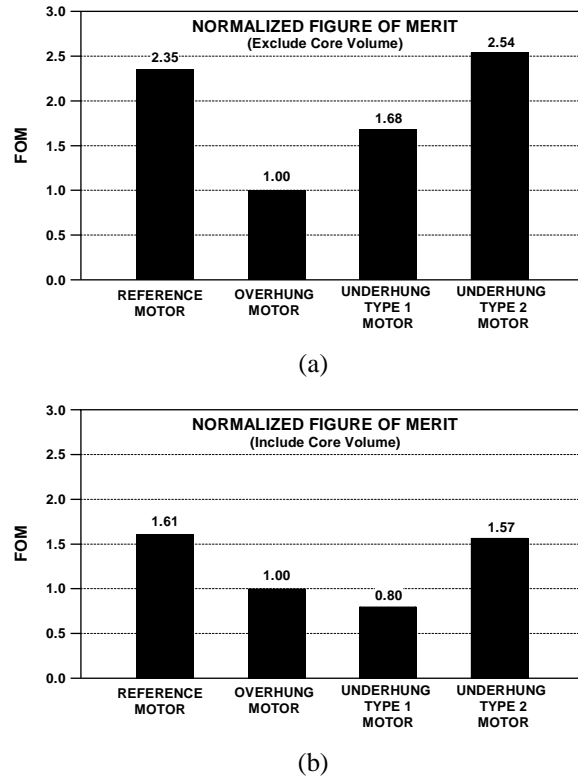


Fig. 8. Figure-of-merit bar charts for the four motor structures analyzed in this addendum (reference, overhung, underhung Type 1, and underhung Type 2). All structures uses identical voice-coils and are designed to have the same BI of 18 T-m. All the motors allow the voice-coil to partially leave the gap so that  $X_{\max}$  is defined at the excursion where the BI drops to a level of 70.7% of the rest-position BI.

## 8. CONCLUSIONS

This addendum added additional information and the results of further research into the claims of Ray Newman's 1992 Electro-Voice memo that extolled the advantages of the underhung loudspeaker motor structure as contrasted to the overhung motor. This additional information and research was not discussed in Ray Newman's original memos, but is reported here as a logical extension of his work. The thermal characteristics of the motors were not considered in the original paper or this addendum.

This addendum added plots of BI versus voice-coil displacement for the three motor structures evaluated in the original paper, defined and analyzed a new type underhung structure where the voice-coil is allowed to partially leave the magnetic gap, and defined a motor structure figure of merit (FOM) that was subsequently applied to all the analyzed motor structures.

The BI versus displacement plots revealed that the underhung motor structure's BI decays much more slowly when the voice-coil leaves the gap as compared to an overhung structure using the same voice-coil and designed to provide the same geometric  $X_{\max}$ . This means that the maximum excursion of the underhung motor is significantly higher than the overhung motor if the maximum displacement is defined at a point where the BI is allowed to drop to a specific level (usually 70.7 or 82% of the rest position BI).

This addendum defined a new type underhung structure that allows the voice-coil to partially leave the gap and categorized the old and new underhung motors as Type 1 and Type 2 respectively.

This addendum also defined a motor structure figure of merit (FOM) that depends on the electro-magnetic damping factor ( $(BI)^2/R_c$ ), maximum excursion ( $X_{\max}$ ), total magnetic energy ( $E_{TM}$ ), and physical core volume ( $V_c$ ). The FOM is directly proportional to the first two parameters and inversely proportional to the last two parameters.

An example underhung Type 2 motor was designed which had an equal maximum excursion as the overhung motor when BI was allowed to sag to 70.7% of the rest-position BI. Both motors used the same voice-coil and had the same rest-position BI. The shape of this motor's BI versus displacement curve was unique in that it had a very flat linear region for small displacements and then rolled off gradually until the BI sags to the 70.7% level.

This addendum analyzed this new motor (underhung Type 2) along with the three motor structures defined in the original paper (reference, overhung, and underhung Type 1), but with the stipulation that voice-coil of all motors be allowed to leave the gap so that  $X_{\max}$  can be defined at the level where BI drops to 70.7% of the rest-position BI.

When the FOM was applied to these four motor structures, several interesting results were revealed:

1. The highest FOMs were exhibited by the reference and underhung Type 2 structures which had roughly equal FOMs.
2. When the core physical volume was excluded from the FOM calculations:
  - a) The overhung motor had the lowest FOM of all the four structures.

- b) The FOMs of the reference and underhung Type 2 motors were roughly 2.5 times higher than the underhung motor with the Type 2 motor's FOM the highest of the four.
  - c) The underhung Type 1 motor had nearly a 70% higher FOM than the underhung structure.
3. When the core physical volume was included in the FOM calculations:
- a) The reference, underhung Type 1, and underhung Type 2 FOMs dropped significantly as compared to the overhung motor.
  - b) The reference and underhung Type 2 motors had roughly the same FOMs but were still about 60% higher than the overhung motor.
  - c) The FOM of the underhung Type 1 motor was about 20% less than the overhung motor.

structures analyzed. This implies that if efficiency and maximum excursion are important, these structures provide the "most bang for the buck."

The new information in this addendum essentially confirms Ray Newman's original claims about the superiority of the underhung loudspeaker motor structure. Although Newman's original claims were just based on analyzing the required magnet energy of a structure that neglected fringe and core magnetic losses (and nearly every other motor parameter), when these losses and other factors are included, such as maximum excursion and physical core volume, the reference and underhung motors still come out on top.

Recommendations and comments (Proviso: this section was written by co-author Keele and may not represent the conclusions of the other co-authors or the companies they represent.):

- If possible, implement your loudspeaker with an underhung rather than an overhung motor structure.
- If motor physical depth and weight are important, such as in automotive applications, the overhung motor may be the best choice.
- The underhung Type 1 motor structure can provide an extremely linear BI versus displacement characteristic for all voice-coil displacements. This makes it an ideal choice for applications where low distortion is important.
- The underhung Type 2 structure provides a very linear BI versus displacement attribute for small displacements with a gradual roll off for higher displacements. This is often a very good match to typical bass program material that exhibits an amplitude histogram that spends most of its time around low amplitude values.
- The reference and underhung Type 2 motor structures both have the highest FOM of all the

Table 1: Motor Structure Simulation Data, CASE 3 (Constant BI Product = 18.0 T·m, n = 300 turns)

Motor	MMF	Average Flux Density in Gap, B	BI Force Factor	Core Flux	Core Physical Volume (Relative to Overhung Structure value of 0.568 x 10 <sup>-3</sup> m <sup>3</sup> )	Reluctance			Magnetic Energy			
						Gap	Core	Total	Gap	Core	Fringe	Total
Reference	522	0.252	18.144	2.30	1.46	0.221	0.006	0.227	0.588	0.0114	0.10	0.70
Overhung	1,494	0.715	18.080	1.30	1.00	1.137	0.012	1.149	0.999	0.0137	1.03	2.04
Underhung Type 1	2891	0.250	18.035	4.10	2.11	0.123	0.582	0.705	1.043	0.8645	0.133	2.04
Underhung Type 2, 70% BI	548	0.248	17.902	3.05	1.62	0.164	0.016	0.180	0.685	0.0221	0.096	0.803

Table 2: Motor Structure  $X_{\max}$ , and Figure of Merit for the Geometric  $X_{\max}$  Designs (CASE 3:  $Bl = 18 \text{ T}\cdot\text{m}$ )

Motor	$X_{\max}$	Figure of Merit (Without Core Volume) (Normalized to Overhung Structure)	Figure of Merit (With Core Volume) (Normalized to Overhung Structure)
	Inches	$FM = \frac{(Bl)^2}{R_e} \cdot \frac{1}{\text{TotalEnergy}} \cdot \frac{1}{\text{CoreVolume}} \cdot X_{\max}$	$FM = \frac{(Bl)^2}{R_e} \cdot \frac{1}{\text{TotalEnergy}} \cdot X_{\max}$
Reference	0.000	0.00	0.00
Overhung	0.600	1.00	1.00
Underhung Type 1	0.600	1.00	0.47

Table 3: Motor Structure  $X_{\max}$ , and Figure of Merit for the 70%  $Bl$  Droop Designs (CASE 3:  $Bl = 18 \text{ T}\cdot\text{m}$ )

Motor	$X_{\max}$	Figure of Merit (Without Core Volume) (Normalized to Overhung Structure)	Figure of Merit (With Core Volume) (Normalized to Overhung Structure)
	Inches	$FM = \frac{(Bl)^2}{R_e} \cdot \frac{1}{\text{TotalEnergy}} \cdot X_{\max}$	$FM = \frac{(Bl)^2}{R_e} \cdot \frac{1}{\text{TotalEnergy}} \cdot \frac{1}{\text{CoreVolume}} \cdot X_{\max}$
Reference	0.546	2.35	1.61
Overhung	0.678	1.00	1.00
Underhung Type 1	1.140	1.68	0.80
Underhung Type 2	0.678	2.54	1.57

## 9. REFERENCES

- [1] W. Klippel, "Assessment of Voice-Coil Peak Displacement  $X_{\max}$ ," J. Audio Eng. Soc., vol. 51, no. 5, pp. 307-323, (2003 May).